LETTERS

# Self-destructive cooperation mediated by phenotypic noise

Martin Ackermann[1], Bärbel Stecher[2], Nikki E. Freed[1], Pascal Songhet[2], Wolf-Dietrich Hardt[2] & Michael Doebeli[3]

**In many biological examples of cooperation, individuals that cooperate cannot benefit from the resulting public good. This is especially clear in cases of self-destructive cooperation, where individuals die when helping others. If self-destructive cooperation is genetically encoded, these genes can only be maintained if they are expressed by just a fraction of their carriers, whereas the other fraction benefits from the public good. One mechanism that can mediate this differentiation into two phenotypically different sub-populations is phenotypic noise[1,2]. Here we show that noisy expression of self-destructive cooperation can evolve if individuals that have a higher probability for self-destruction have, on average, access to larger public goods. This situation, which we refer to as assortment, can arise if the environment is spatially structured. These results provide a new perspective on the significance of phenotypic noise in bacterial pathogenesis: it might promote the formation of cooperative sub-populations that die while preparing the ground for a successful infection. We show experimentally that this model captures essential features of *Salmonella typhimurium* pathogenesis. We conclude that noisily expressed self-destructive cooperative actions can evolve under conditions of assortment, that self-destructive cooperation is a plausible biological function of phenotypic noise, and that self-destructive cooperation mediated by phenotypic noise could be important in bacterial pathogenesis.**

Recent experimental work demonstrated that genetically identical organisms living in the same environment show surprisingly high levels of variation in phenotypic traits[1,2], and sometimes even switch between distinct phenotypic states[3]. Stochastic cellular processes are one source of such phenotypic noise. The level of phenotypic noise is subject to mutational change, and can thus evolve. This raises the question whether natural selection always acts towards minimizing phenotypic noise, or whether there are cases in which genotypes that encode variable phenotypes are favoured by selection. In the existing theory[4–6], the most prominent adaptive explanation for phenotypic noise is bet-hedging[5], according to which the stochastic expression of alternative phenotypes allows a genotype to survive changes in external conditions and thus to persist in fluctuating environments.

Here we focus on a fundamentally different adaptive explanation for phenotypic noise: self-destructive cooperation. In this scenario, the individuals that survive and form a successful lineage all express the same phenotype. Individuals that express an alternative phenotype do exist, but they do not contribute to future generations; instead, they die while contributing to a public good that benefits others. There are many examples of cooperative acts that prevent reproduction or survival of the actor, ranging from non-reproductive workers in mammals and insects to unicellular bacteria that lyse when releasing chemical substances that benefit others. Importantly, genotypes that have the propensity to express self-destructive cooperation can only persist if the expression is limited to a fraction of the individuals carrying the genotype, whereas another fraction does not express the cooperative behaviour and benefits from the public good produced. Sometimes, this differentiation into two fractions is mediated by signals. In other examples, notably in microorganisms, there seems to be no signal. In these cases, phenotypic noise could promote the differentiation required for self-destructive cooperation to persist.

We investigated the evolutionary dynamics of a self-destructive cooperative act that contributes to the generation of a public good and that is expressed in a stochastic manner. In general, cooperation can evolve if cooperative individuals benefit from cooperative acts of others more often than non-cooperative individuals[7]—a situation referred to as assortment. We used a simple model to quantify the level of assortment as a function of the external conditions, and to calculate how selection on the probability to express self-destructive cooperation depends on the level of assortment, as well as on the amount of public good generated by cooperative acts.

The model is based on the public goods game and assumes that there are two strategies: cooperate (C) and defect (D). C sacrifices itself with probability $q$, and only if it sacrifices itself, it contributes an amount $b$ to the public good. The decision between sacrificing and not sacrificing is a chance outcome resulting from phenotypic bistability; every cooperator makes this decision independently of the environment or of the decisions of other individuals. D never contributes to the public good. The game is played in interaction groups of $N$ players. In general, if there are $k$ cooperators among the $N$ members of an interaction group, the total amount of the public good produced in that group is $kqb$. The total amount of the public good is available to each surviving player in the interaction group (an alternative scenario where the public good is divided among the surviving players gives very similar results). We assume that, in addition to the public good, all players also receive a non-zero baseline payoff $w$.

Consider first the payoff to a focal C player in a given interaction group. Because the focal C is one of the $k$ cooperators, its social environment consists of $k-1$ cooperators and $N-k$ defectors. The focal C gets no payoff from the defectors, but if it survives it receives the benefit $b$ with a probability $q$ from each of the other $k-1$ cooperators, as well as the baseline payoff $w$. The probability that the focal C does not sacrifice itself is $1-q$, and hence the expected payoff to C in the given interaction group is:

$$p_C(N,k) = (1-q)((k-1)qb+w) \quad (1)$$

The social environment of a focal D in the given interaction group consists of $k$ cooperators and $N-k-1$ defectors, and its expected payoff is:

[1]Institute of Integrative Biology, ETH Zurich, 8092 Zürich, Switzerland. [2]Institute of Microbiology, ETH Zurich, 8093 Zürich, Switzerland. [3]Department of Zoology and Department of Mathematics, University of British Columbia, Vancouver BC V6T 1Z4, Canada.

$$p_D(N,k) = kqb + w \quad (2)$$

Because $p_C(N,k) < p_D(N,k)$, cooperators always do worse than defectors within a given group. Therefore, the only way in which cooperators can dominate on a population-wide scale is if cooperators have, on average, a different social environment than defectors.

The composition of the social environment of a focal C or D depends on the current frequency of cooperators in the population, $x$, and on how individuals come together to form interaction groups. Let $e_C(x)$ be the average number of cooperators among the other $N-1$ members in an interaction group containing a focal C. Similarly, let $e_D(x)$ be the number of cooperators in an average interaction group containing a focal D. The expected population-wide payoffs to C and D are then:

$$P_C(x) = (1-q)(e_C(x)qb + w) \quad (3)$$

and

$$P_D(x) = e_D(x)qb + w \quad (4)$$

With random composition of groups, we have $e_C(x) = e_D(x) = x(N-1)$. In this case, the population-wide payoffs always satisfy $P_C(x) < P_D(x)$ for all $x$, and hence defectors always win. Thus, for cooperation to thrive, cooperators must find themselves, on average, in interaction groups containing more cooperators than the interaction groups in which defectors find themselves on average. In other words, there must be positive assortment between cooperators.

Assortment can result from different mechanisms, for example, spatial structure, reciprocity or kin recognition[7]. Here we consider a simple case of spatially structured populations inhabiting an infinite number of demes. In the case of pathogenic bacteria, a deme would represent a host. Each deme is seeded by $M$ individuals from a common pool of individuals. The number of individuals then increases to the carrying capacity of the deme, which is assumed to be $N$, the interaction group size. After reaching carrying capacity, cooperators sacrifice themselves with probability $q$; if they do, they contribute $b$ to the public good. Cooperators that did not sacrifice themselves and defectors then harvest the public good. The payoffs they receive determine how much they contribute to the pool of individuals from which the next generation of demes is seeded.

If the number of individuals seeding a deme, $M$, is small, then the degree of assortment is high, and a focal cooperator sees on average more cooperators than a focal defector. It is easy to see (see Supplementary Information) that the average social environment of a focal cooperator and a focal defector is:

$$e_C(x) = \frac{(M-1)N}{M}x + \frac{N}{M} - 1 \quad (5)$$

and

$$e_D(x) = \frac{(M-1)N}{M}x \quad (6)$$

Thus, $e_C(x) > e_D(x)$ for all $x$, which enables the origin and maintenance of cooperation based on equations (3) and (4). The general picture is as follows (Fig. 1; derivation in Supplementary Information): First, there is a value $q_1^*$ such that for any $q < q_1^*$, C can invade D, that is, $P_C(0) > P_D(0)$ $(q_1^* = [b(N-M) - Mw]/[b(N-M)]$; see Supplementary Information). Second, there is a value $q_2^* < q_1^*$ such that for any $q < q_2^*$, C not only invades D but also goes to fixation, that is, $P_C(1) > P_D(1)$ $(q_2^* = [b(N-M) - Mw]/[b(NM-M)]$; see Supplementary Information). Third, for any $q$ with $q_2^* < q < q_1^*$, there is coexistence between cooperators and defectors, that is, C can invade D and D can invade C.

These results show that the assortment generated by the deme structure changes the nature of the evolutionary game between cooperators and defectors. In well-mixed populations without demes, D always dominates C. With demes, this remains true if C players have large probabilities $q$ of committing cooperative suicide. However, for intermediate $q$ (that is, $q_2^* < q < q_1^*$), the structure of the game changes to a 'Snowdrift' scenario[8], in which both C and D can invade when rare. For even smaller $q$ $(q < q_2^*)$, assortment makes C the dominant strategy and eliminates D.

Defectors D can be viewed as cooperators with $q = 0$, which naturally leads to the consideration of $q$ as a continuous trait. Evolution of such continuous traits can be studied using adaptive dynamics theory[9–11]. Starting with a population of defectors, the trait $q$ evolves to a convergence stable and evolutionarily stable strategy $q_3^*$ satisfying $0 < q_3^* < q_2^*$ $(q_3^* = [b(N-M) - Mw]/[b(NM+N-2M)]$; see Supplementary Information). Therefore, continuous evolution by small steps results in a population consisting of a single cooperative strategy that cannot be invaded by any nearby strategies $q$ or by pure defectors. Our model thus provides a framework for understanding the evolution of self-destructive cooperation mediated by phenotypic noise. We note that our deme-structured model of cooperative suicide can also be interpreted in the context of kin or group selection[7,12]. However, these perspectives are not required for understanding the evolution of cooperation; simple considerations based on assortment and interaction environments are sufficient.

This model sheds new light on the role of phenotypic noise in the biology of microbial pathogens. Phenotypic noise or bi-stability is common in unicellular pathogens, as are acts of self-destructive cooperation[13]. Some bacterial toxins that are instrumental in pathogenesis can only be released if the cell producing the toxin lyses[14–16]. Some of these toxins induce inflammation in the host, and there is now growing evidence that pathogens can decrease competition by co-inhabitants of the same niche through manipulation of the host's immune system[17–20]. One example is pneumolysin from *Streptococcus*

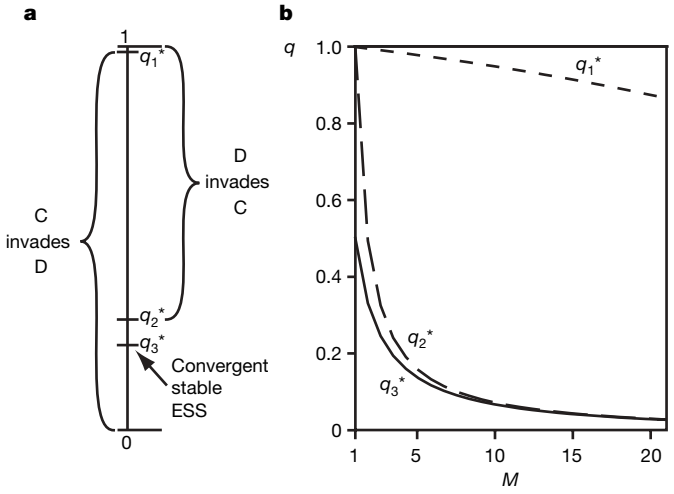


**Figure 1 | The evolutionary dynamics of stochastic self-destructive cooperation. a**, The dynamics are determined by three specific values for the probability $q$ to self-sacrifice. The first value is $q_1^*$. A population of pure defectors can be invaded by cooperators' that self-sacrifice with a probability $q < q_1^*$. The second value is $q_2^*$. A homogeneous population of cooperators can be invaded by defectors if the cooperators' probability to self-sacrifice is larger than $q_2^*$. Cooperators with a probability to self-sacrifice between $q_1^*$ and $q_2^*$ will thus stably co-exist with pure defectors. If $q$ evolves through mutations of small effects, and the population initially consists of defectors, then $q$ will evolve to the value $q_3^*$. This value is an evolutionarily stable strategy (ESS) and represents an endpoint for the evolutionary dynamics. The three values for $q$ are determined by the parameters $M$, $N$, $b$ and $w$, as described in the Supplementary Information. In the example shown here, the parameters are $M = 3$, $N = 100$, $b = 5$ and $w = 2$. **b**, When the number of individuals colonizing a deme, $M$, increases, and assortment therefore decreases, the three values $q_1^*$, $q_2^*$ and $q_3^*$ decrease. The parameter values are $N = 100$, $b = 5$ and $w = 2$.

*pneumoniae*. This toxin is released through bacterial lysis and enhances lung colonization[14,21]. A second example is TcdA, a key virulence factor of *Clostridium difficile*[16]. TcdA lacks a standard secretion signal and is released by bacterial lysis. Purified TcdA toxin alone can trigger gut inflammation[22], and gut inflammation enhances intestinal *C. difficile* colonization[23]. In this case, TcdA released by self-destructive acts seems to provide the pathogen with a competitive advantage, presumably by decreasing competition from commensal bacteria.

We focused on *S. typhimurium* enterocolitis as a third example of bacterial pathogenesis, and tested experimentally whether central aspects of the infection process are captured by the model of self-destructive cooperation mediated by phenotypic noise. The establishment of *S. typhimurium* in the gut is hindered by the presence of the intestinal microflora. These competitors are removed by an inflammatory response in the gut triggered by *S. typhimurium* invading the gut tissue[24]. Gut tissue invasion and the triggering of inflammation depend on *S. typhimurium* virulence factors, namely Type III secretion systems (TTSS) and flagella. Invasion factors—that is, the invasion-mediating TTSS-1 and the flagella—are heterogeneously expressed in *S. typhimurium* populations[25–27]. In our experiments, gut inflammation, which alleviates competition by commensals, was regarded as the public good. We focused on TTSS-1 expression as the phenotypic trait that is expressed stochastically, and tested three main assumptions of the mathematical model (Fig. 2; see Supplementary Information for experimental methods).

Our experimental results show that: first, in a clonal population of *S. typhimurium*, in the gut lumen, only about 15% were phenotypically TTSS-$1^+$, which is in line with *in vitro* studies[26,27]. In contrast, almost all bacteria in the gut tissue expressed the TTSS-$1^+$ phenotype (Fig. 2a,b). This supports the assumption that TTSS-1 expression is variable in clonal populations of *S. typhimurium*, and that the TTSS-1 phenotype of a bacterium determines whether or not it will invade the gut tissue. (Other invasion factors probably also have an important role; TTSS-1 expression is therefore required but not sufficient for invasion.) Second, the intensity of inflammation increases as the proportion of bacteria that are capable of expressing the cooperative TTSS-$1^+$ phenotype increases (Fig. 2c,d). Taking inflammation as a proxy for the public good, this supports the assumption that the public good produced increases with increasing numbers of cooperators. Third, in the *S. typhimurium* enterocolitis model, most of the bacteria that invade the gut tissue and thereby contribute to the public good seem to be killed by the intestinal innate immune defenses (Fig. 2e, f). Thus, cooperation through invasion of the gut tissue is a largely self-destructive act.

Together, these experimental results indicate that the mathematical model of self-destructive cooperation mediated by phenotypic noise captures central features of *S. typhimurium* enterocolitis. This gives a new perspective on how these and similar pathogens evolve self-destructive cooperative acts to infect their hosts. Our model predicts that this behaviour can evolve if the number of pathogens that infect a host is small. This number corresponds to the parameter *M*, and if *M* is small then bacteria that carry the genotype for stochastic cooperation without expressing this behaviour are surrounded by many cells with the same genotype that do cooperate, and hence this genotype will thrive. A first estimate for *M* is the number of bacteria required for an infection to establish. For *Salmonella* spp. and *Escherichia coli* infecting humans, estimates can reach levels as low as one hundred[28]. Mortality during the passage through the stomach, as well as spatial structure of the environment from which the inoculum originates, can lead to a small effective *M* even if the infective dose is substantial. Over evolutionary time, a small *M* leads to the evolution of larger probabilities to express the cooperative act (Fig. 1) and, as one can easily show mathematically, to larger payoffs. This is in line with previous theoretical findings that clonal infections are beneficial for pathogens, whereas coinfection tends to be detrimental[29].

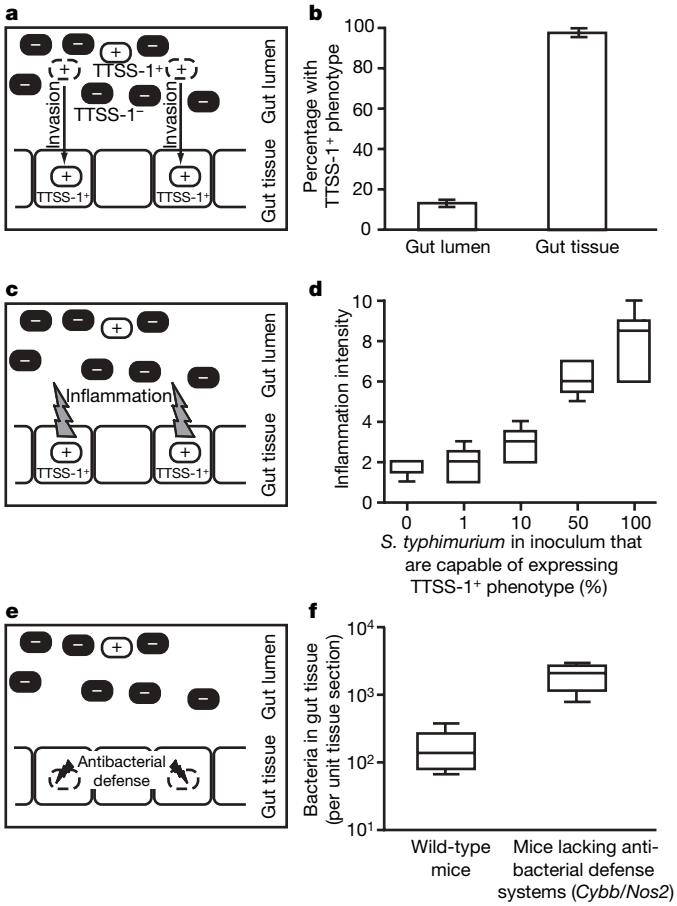


**Figure 2 | Testing biological assumptions of self-destructive cooperation mediated by phenotypic noise with a mouse model for *S. typhimurium* enterocolitis.** For experimental details, see Supplementary Information. **a**, The clonal bacterial population consists of two phenotypes; one of them (TTSS-$1^+$; white) expresses a cooperative act consisting of gut tissue invasion. **b**, We analysed the TTSS-1 phenotype in the gut lumen and in the gut tissue. In the gut lumen, about 15% of the bacteria were TTSS-$1^+$; in the gut tissue, almost all bacteria were TTSS-$1^+$ (Mann–Whitney U test for a difference between lumen and tissue, $P < 0.001$; error bars, s.e.m.). The luminal *S. typhimurium* population differentiates into TTSS-$1^+$ and TTSS-$1^-$ phenotypes, and the TTSS-$1^+$ phenotype invades the gut tissue. **c**, The amount of public good generated in an interaction group increases with an increasing number of cooperators. In the context of *S. typhimurium* infection, the public good is gut inflammation elicited by tissue invasion. **d**, To vary the number of bacteria that commit the cooperative act, we mixed wild-type *S. typhimurium* that express both TTSS-$1^+$ and TTSS-$1^-$ phenotypes (see **b**) with an isogenic strain that is incapable of expressing the TTSS-$1^+$ phenotype (ΔTTSS-1). The intensity of gut inflammation increased with an increasing fraction of wild-type *S. typhimurium* in the inoculum (box plots with median, quartiles and range; Spearman's rank correlation, $P < 0.001$). Gut inflammation increases with an increasing number of individuals that express the cooperative act of tissue invasion. **e**, Contributing to the public good is a self-destructive act. In the context of *S. typhimurium* infection, most bacteria invading the gut tissue are expected to be killed by antimicrobial defence mechanisms, specifically by the *Cybb*/*Nos2*-encoded systems generating antimicrobial oxygen and nitrogen radicals. **f**, To test whether bacteria that invade the gut tissue are killed, we compared *S. typhimurium* loads in the gut tissue of wild-type mice and of mutant mice lacking the *Cybb*/*Nos2* systems. The bacterial loads in the gut tissue in wild-type mice were about ten times lower than in the *Cybb*/*Nos2*-knockout mice (box plots with median, quartiles and range; Mann–Whitney U test, $P = 0.008$; in the gut lumen, bacterial loads were not significantly different; see Supplementary Information). This suggests that in wild-type mice, most bacteria that invade the gut tissue are killed. Thus, triggering of gut inflammation by tissue invasion can be regarded as a self-destructive act.

Self-destructive cooperation can be seen as an extreme form of the division of labour between two phenotypes, in which one of the phenotypes does not survive. The two phenotypes are encoded by the same genotype, which can persist because the expression of the self-destructive phenotype is stochastic. We thus conclude that self-destructive cooperation is a plausible biological explanation for certain instances of phenotypic noise. Establishing a link between phenotypic noise and cooperation gives new insights into how cooperation can persist despite its cost for the benefactor. At the same time, this link provides a new perspective into the significance of phenotypic noise in biological systems, and especially in microbial pathogens. Understanding why so many pathogens exhibit stochastic phenotypic variation is essential for developing efficient strategies for their control.

**Received 13 March; accepted 6 May 2008.**


1. Raser, J. M. & O'Shea, E. K. Noise in gene expression: origins, consequences, and control. *Science* **309,** 2010–2013 (2005).
2. Kaern, M., Elston, T. C., Blake, W. J. & Collins, J. J. Stochasticity in gene expression: from theories to phenotypes. *Nature Rev. Genet.* **6,** 451–464 (2005).
3. Dubnau, D. & Losick, R. Bistability in bacteria. *Mol. Microbiol.* **61,** 564–572 (2006).
4. Bull, J. J. Evolution of phenotypic variance. *Evolution* **41,** 303–315 (1987).
5. Kussell, E., Kishony, R., Balaban, N. Q. & Leibler, S. Bacterial persistence: a model of survival in changing environments. *Genetics* **169,** 1807–1814 (2005).
6. Wolf, D. M., Vazirani, V. V. & Arkin, A. P. A microbial modified prisoner's dilemma game: how frequency-dependent selection can lead to random phase variation. *J. Theor. Biol.* **234,** 255–262 (2005).
7. Nowak, M. A. Five rules for the evolution of cooperation. *Science* **314,** 1560–1563 (2006).
8. Hauert, C. & Doebeli, M. Spatial structure often inhibits the evolution of cooperation in the snowdrift game. *Nature* **428,** 643–646 (2004).
9. Nowak, M. & Sigmund, K. The evolution of stochastic strategies in the Prisoner's Dilemma. *Acta Appl. Math.* **20,** 247–265 (1990).
10. Dieckmann, U. & Law, R. The dynamical theory of coevolution: a derivation from stochastic ecological processes. *J. Math. Biol.* **34,** 579–612 (1996).
11. Metz, J. A. J., Geritz, S. A. H., Meszena, G., Jacobs, A. & van Heerwaarden, J. S. in *Stochastic and Spatial Structures of Dynamial Systems* (eds van Strien, S. J. & Verduyn, S. M.) 183–231 (North Holland, Amsterdam, 1996).
12. Charlesworth, B. Some models of the evolution of altruistic behaviour between siblings. *J. Theor. Biol.* **72,** 297–319 (1978).
13. Avery, S. V. Microbial cell individuality and the underlying sources of heterogeneity. *Nature Rev. Microbiol.* **4,** 577–587 (2006).
14. Paton, J. C. The contribution of pneumolysin to the pathogenicity of *Streptococcus pneumoniae*. *Trends Microbiol.* **4,** 103–106 (1996).
15. Wagner, P. L. *et al.* Bacteriophage control of Shiga toxin 1 production and release by *Escherichia coli*. *Mol. Microbiol.* **44,** 957–970 (2002).
16. Voth, D. E. & Ballard, J. D. *Clostridium difficile* toxins: mechanism of action and role in disease. *Clin. Microbiol. Rev.* **18,** 247–263 (2005).
17. Lysenko, E. S., Ratner, A. J., Nelson, A. L. & Weiser, J. N. The role of innate immune responses in the outcome of interspecies competition for colonization of mucosal surfaces. *PLoS Pathog* **1,** e1 (2005).
18. Raberg, L. *et al.* The role of immune-mediated apparent competition in genetically diverse malaria infections. *Am. Nat.* **168,** 41–53 (2006).
19. Brown, S. P., Le Chat, L. & Taddei, F. Evolution of virulence: triggering host inflammation allows invading pathogens to exclude competitors. *Ecol. Lett.* **11,** 44–51 (2007).
20. Stecher, B. & Hardt, W.-D. The role of microbiota in infectious disease. *Trends Microbiol.* **16,** 107–114 (2008).
21. Ogunniyi, A. D., Grabowicz, M., Briles, D. E., Cook, J. & Paton, J. C. Development of a vaccine against invasive pneumococcal disease based on combinations of virulence proteins of *Streptococcus pneumoniae*. *Infect. Immun.* **75,** 350–357 (2007).
22. Lima, A. A. M., Lyerly, D. M., Wilkins, T. D., Innes, D. J. & Guerrant, R. L. Effects of *Clostridium difficile* toxins A and B in rabbit small and large intestine *in vivo* and on cultured cells *in vitro*. *Infect. Immun.* **56,** 582–588 (1988).
23. Rodemann, J. F., Dubberke, E. R., Reske, K. A., Seo, D. H. & Stone, C. D. Incidence of *Clostridium difficile* infection in inflammatory bowel disease. *Clin. Gastroenterol. Hepatol.* **5,** 339–344 (2007).
24. Stecher, B. *et al. Salmonella enterica* serovar Typhimurium exploits inflammation to compete with the intestinal microbiota. *PLoS Biol.* **5,** e244 (2007).
25. Cummings, L. A., Wilkerson, W. D., Bergsbaken, T. & Cookson, B. T. *In vivo*, fliC expression by *Salmonella enterica* serovar Typhimurium is heterogeneous, regulated by ClpX, and anatomically restricted. *Mol. Microbiol.* **61,** 795–809 (2006).
26. Hautefort, I., Proenca, M. J. & Hinton, J. C. D. Single-copy green fluorescent protein gene fusions allow accurate measurement of *Salmonella* gene expression *in vitro* and during infection of mammalian cells. *Appl. Environ. Microbiol.* **69,** 7480–7491 (2003).
27. Schlumberger, M. C. *et al.* Real-time imaging of type III secretion: *Salmonella* SipA injection into host cells. *Proc. Natl Acad. Sci. USA* **102,** 12548–12553 (2005).
28. Kothary, M. H. & Babu, U. S. Infective dose of foodborne pathogens in volunteers: A review. *J. Food Saf.* **21,** 49–73 (2001).
29. May, R. M. & Nowak, M. A. Coinfection and the evolution of parasite virulence. *Proc. Biol. Sci.* **261,** 209–215 (1995).


**Supplementary Information** is linked to the online version of the paper at www.nature.com/nature.

**Acknowledgements** We are grateful to Markus Schlumberger, K. Aktories, I. Just, S. Hammerschmidt and J. Fletcher for discussions, and M. Barthel and the RCHCI team for professional help with the animal experiments. M.A. and N.E.F. were supported by the Swiss National Science Foundation, and M.A. was also supported by the Roche Research Foundation and the Novartis Foundation. M.D. is supported by NSERC (Canada). B.S. and W.-D.H. were supported by the UBS foundation. *Salmonella* work in the Hardt laboratory is supported by grants from the ETH research foundation (TH-10 06-1), the Swiss National Science Foundation (310000-113623/1) and the European Union (SavinMucoPath number 032296).

**Author Contributions** M.A., W.-D.H. and M.D. formulated the question; M.A. and M.D. wrote the mathematical model; M.D. analysed the mathematical model; M.A., B.S., N.E.F. and W.-D.H. planned the experiments and interpreted the results; B.S. performed the experiments for Fig. 2b, d; P.S. performed the experiment for Fig. 2f; and M.A., W.-D.H. and M.D. wrote the manuscript.

**Author Information** Reprints and permissions information is available at www.nature.com/reprints. Correspondence and requests for materials should be addressed to M.A. (martin.ackermann@env.ethz.ch), W.-D.H. (hardt@micro.biol.ethz.ch) or M.D. (doebeli@zoology.ubc.ca).

# Supplementary Notes for Ackermann et al.

*Part I: Additional mathematical analysis of the model for the evolution of self-destructive cooperation mediated by phenotypic noise*

In the following analysis, we use the within interaction group payoffs given by eqs. (1) and (2) for the case where the public good is fully available to everybody in a given interaction group. The case where the public good is distributed among the surviving members of the interaction group can be analyzed along the same lines, and gives qualitatively very similar results.

We assume that the population is spatially structured as described in the text, and hence that the functions $e_C(x)$ and $e_D(x)$ are given by eqs. (5) and (6). Recall that $e_C(x)$ and $e_D(x)$ are the average number of cooperators in an interaction group of a focal $C$ or $D$, respectively, when the population frequency of $C$ is $x$.

We want to investigate invasion of $C$ into a population of $D$ and vice versa, hence we consider the cases $x = 0$ and $x = 1$. When $C$ is rare, we have $e_C(0) = N/M - 1$ and $e_D(0) = 0$, hence

$$P_C(0) = (1 - q)\left(\frac{(N - M)qb}{M} + w\right) \tag{1}$$

and

$$P_D(0) = w. \tag{2}$$

$C$ can invade $D$ if and only if $P_C(0) > P_D(0)$, which is the case if and only if $q < q_1^*$, where $q_1^*$ is given by

$$q_1^* = \frac{b(N - M) - Mw}{b(N - M)}. \tag{3}$$

Thus, cooperators can invade defectors at least for some $q$ if $\frac{w}{b} < \frac{N-M}{M}$. In particular, smaller baseline fitness $w$, larger benefit to cooperation $b$, larger interaction group size $N$ and smaller neighborhood size $M$ (i.e., more pronounced spatial structure) are all beneficial for cooperation, which makes sense intuitively.

Similarly, $D$ can invade $C$ if and only if $P_C(1) < P_D(1)$, which is the case if and only if $q > q_2^*$, where $q_2^*$ is given by

$$q_2^* = \frac{b(N-M) - Mw}{b(NM-M)}. \tag{4}$$

Thus, for $q < q_2^*$, $D$ cannot invade $C$. Clearly, $q_2^* < q_1^*$, hence for $q < q_2^*$, $C$ can invade $D$, but $D$ cannot invade $C$. It is easy to see that this in turn implies that for $q < q_2^*$, $C$ replaces $D$, whereas for $q_2^* < q < q_1^*$, the two strategies can invade each other and hence they coexist at a mixed equilibrium. This proves claims 1)-3) in the main text.

To investigate the adaptive dynamics of the continuous trait $q$, we consider resident populations that are monomorphic for a particular trait value $q$ into which a rare mutant with a mutant trait value $q'$ attempts to invade. Because the mutant is rare, and given the spatial structure described in the main text, the environment of the mutant in an interaction group of size $N$ consists of $N/M - 1$ mutant types $q'$ and $N(M-1)/M$ resident types $q$. Thus, the payoff of the mutant $q'$ in the resident $q$, which is the *invasion fitness* of the mutant $q'$, is given by

$$f(q,q') = \left( \frac{(N-M)q'b}{M} + \frac{N(M-1)qb}{M} + w \right)(1-q'). \tag{5}$$

The adaptive dynamics is then given by the selection gradient

$$D(q) = \frac{\partial f(q,q')}{\partial q'}|_{q'=q} = \frac{b\left(N(1-q) - M(1-2q+Nq)\right)}{M} - w. \tag{6}$$

For any given resident value $q$, the direction of evolution is determined by the sign of $D(q)$. In particular, if $w < b(N-M)/M$, then $D(0) > 0$, and hence the trait $q$ evolves away from $0$. (Note that this is the same condition as the condition for $q_1^* > 0$, and hence for the existence of a range of $q$-values for which cooperators can invade pure defectors.) In this case, the function $D(q)$ is linear with a negative slope. Therefore, the equation $D(q) = 0$ has a unique, positive solution

$$q_3^* = \frac{b(N-M) - Mw}{b(MN+N-2M)}, \tag{7}$$

and $q_3^*$ is a global attractor of the adaptive dynamics (i.e., starting with any $q_0$ in the interval $[0,1]$, the adaptive dynamics converges to $q_3^*$). Moreover, one easily checks that

$$\frac{\partial^2 f(q,q')}{\partial q'^2}|_{q'=q=q_3^*} = -\frac{2b(N-M)}{M} < 0, \tag{8}$$

and hence $q_3^*$ is evolutionarily stable. It is again clear from direct comparison of the denominators that if cooperation can persist, i.e., if $w < b(N-M)/M$, then $q_3^* < q_2^*$. This means that the evolutionary dynamics comes to a halt before the probability to sacrifice is so high that pure defectors can invade and coexist with cooperators. Thus, continuous evolution in small steps (as is assumed in the adaptive dynamic framework) results in a population consisting of a single cooperative strategy.

To illustrate the change in the nature of the evolutionary game between $C$ and $D$ brought about by assortment due to spatial structure, consider the case $M = 2$, in which each local deme is seeded by 2 individuals, so that there are three types of demes: $CC$, $CD$ and $DD$. In this case the game between cooperators and defectors can be viewed as a classical 2x2 game with two players and two strategies $C$ and $D$. If a focal $C$ colonizes a deme containing another $C$-seed, the payoff to the focal $C$-strategy will be $P_{CC} = (1-q)[(N-1)bq + w]$, and if the focal $C$ colonizes a deme in which the other seed is a $D$, then the payoff to the focal $C$-strategy is $P_{CD} = (1-q)[(N/2-1)bq + w]$. Similarly, the payoff for focal $D$ players are $P_{DC} = (n/2-1)bq + w$ and $P_{DD} = w$, depending on whether the other seed in the deme is a $C$ or a $D$. In general, replicator dynamics of 2x2-games have three outcomes[30]: i) there are only the two boundary equilibria, and one strategy always dominates the other; ii) there is a stable interior equilibrium, at which the two strategies coexist; and iii) there is an unstable interior equilibrium, in which case one strategy wins, but the winner depends on initial conditions. In our model, case iii) does not occur. Instead, with $M = 2$ and the payoffs $P_{CC}$, $P_{CD}$, $P_{DC}$ and $P_{DD}$ given above, case i) holds with $D$ the dominant strategy if $P_{CD} < P_{DD}$ and $P_{CC} < P_{DC}$, which occurs if and only if $q > q_1*$, where $q_1^*$ is given by eq. (9) for $M = 2$. If $q_2^* < q < q_1^*$, with $q_2^*$ given by eq. (10), the payoffs satisfy $P_{CD} < P_{DD}$ and $P_{CC} > P_{DC}$, which generates scenario ii) and leads to coexistence of $C$ and $D$. This situation corresponds to the well-known Snowdrift game[8]. Finally, case i) with $C$ the dominant strategy occurs for $q < q_2^*$, for which $P_{CD} > P_{DD}$ and $P_{CC} > P_{DC}$. Overall, for $q < q_1^*$ assortment through spatial structure changes the nature of the game between $C$ and $D$ compared to the dominance of $D$ observed in well-mixed populations. For $M > 2$, the effect of assortment on the game between $C$ and $D$ can be similarly understood in a general framework for $N$-player games[31].

*Part II: Additional information on the mouse infection experiments with S. typhimurium.*

**Experiment 1; Analyzing the TTSS-1 expression phenotype of individual bacteria in the gut lumen and the gut tissue in a mouse infection experiment (Figure 2b of the paper).**

Under in vitro culture conditions, 10-30% of a clonal wild type *S. typhimurium* population expresses the TTSS-$1^+$ phenotype, and the rest is TTSS-$1^-$ ([32,33]). We employed an animal model for *S. typhimurium* enterocolitis ([34]; reviewed in[35]) to analyze whether TTSS-$1^+$ and TTSS-$1^-$ subpopulations also exist in vivo. In addition, we wanted to verify that only the TTSS-$1^+$ subpopulation invades into the gut tissue.

Streptomycin-treated C57BL/6 mice were infected as described[34] with wild type *S. typhimurium* (SL1344; 5 * $10^7$ cfu, intragastrically; n = 3 mice). The bacteria carried two reporter plasmids. pM974 allowed detecting TTSS-$1^+$ bacteria. It encodes a GFP-reporter coupled to the TTSS-1 promoter of the *sicAsipBCDA* operon. The second plasmid, pDsRed, leads to bright red fluorescence in all bacteria located in intestinal tissues[36]. The mice were sacrificed at 12 hours post infection. Earlier work has indicated that 12h is long enough to allow significant tissue invasion by *S. typhimurium*. At the same time it is short enough to avoid pronounced bacterial growth within the host tissue which may have diluted out the TTSS-1-GFP signal. We determined total colonization levels of *S. typhimurium* in the gut lumen by plating appropriate dilutions of the cecal contents on McConkey agar. The density of bacteria was 2.1 x $10^9$ +/- 2.5 x $10^8$ (cfu/gram, +/-standard error). In addition, we analyzed gut inflammation using hematoxilin and eosin stained cecum tissue sections and a scoring scheme as described previously[37]. The average inflammation intensity was 5 +/- 1.7 (mean +/-standard error or the mean). This corresponds to a strong, acute gut inflammation.

The results obtained by analyzing TTSS-$1^+$ (i.e. GFP-) expression in individual *S. typhimurium* bacteria localized in the gut lumen or in the cecal tissue are depicted in Figure 2b. These data were obtained in the following way: Cecal tissue was fixed and embedded to

preserve and visualize GFP and DsRed fluorescence as described previously[37]. For analyzing TTSS-1$^+$ (i.e. GFP-) expression in the cecum tissue, tissue sections (20µm) were stained with phalloidin-Alexa-647 (infrared fluorescence; stains the actin brush border of the epithelium) and DAPI (4' 6'–diamidino-2-phenylindole, 0.5µg/ml, Sigma; blue fluorescence; stains DNA). Confocal images of individual bacteria inside of the cecum tissue (bright DsRed fluorescence) were analyzed using a Perkin Elmer Ultraview confocal imaging system and a Zeiss Axiovert 200 microscope. We identified a total of 87 individual *S. typhimurium* bacteria in the cecum tissues from the 3 mice (three 20 µm thick tissue slices per mouse) and 86 of the 87 bacteria harboured significant levels of the GFP reporter, indicating that these cells express TTSS-1 (Figure 2b).

TTSS-1 expression by luminal bacteria was analyzed in the same way. However, bacteria were stained additionally with an anti-*S. typhimurium* antiserum (polyclonal rabbit α-LPS O antigen group B anti-serum; Difco; 1:500 in PBS, 10% goat serum) and a Cy3-conjugated goat α-rabbit antibody (Milan; 1:300 in PBS, 10% goat serum; red fluorescence) to enhance sensitive and specific detection of *S. typhimurium* in the gut lumen. At least 100-300 individual bacteria (red$^+$) were scored per mouse. The fraction of luminal bacteria (open bars) expressing the GFP-reporter (= TTSS-1$^+$ phenotype) was calculated as: GFP$^+$red$^+$[%] = #GFP$^+$red$^+$/(#GFP$^+$red$^+$ + #GFP$^-$red$^+$) x 100. Approximately 15% of the luminal *S. typhimurium* population expressed the TTSS-1$^+$ phenotype (Figure 2b).

**Experiment 2. Analyzing how decreasing factions of wild type *S. typhimurium* affect the elicitation of gut inflammation in mouse infection experiments (Figure 2d of the paper and suppl. Fig. S1).**

In the streptomycin mouse model, wild type *S. typhimurium* efficiently colonizes the large intestinal lumen and triggers pronounced gut inflammation within one day post infection[34]. An isogenic *S. typhimurium* mutant carrying a mutation disrupting TTSS-1 function (ΔTTSS-1, i.e. SB161; Δ*invG*) is still able to efficiently colonize the gut lumen, but it cannot

efficiently invade the gut tissue and it is incapable of triggering inflammation at day one post infection[34 38].

In the gut lumen, 15% of the wild type *S. typhimurium* population expresses the TTSS-1$^{+}$ phenotype. In contrast, the gut luminal ΔTTSS-1 population never expresses the TTSS-1$^{+}$ phenotype. Therefore, infections with mixtures of wild type *S. typhimurium* and ΔTTSS-1 result in a proportional decrease in the total number of bacteria expressing the TTSS-1$^{+}$ phenotype in the gut lumen.

Streptomycin treated mice (n = 10 C57BL/6 mice per group) were infected intragastrically with a total of 5 * $10^7$ bacteria. This inoculum was composed of either 100% ΔTTSS-1, 1% wild type *S. typhimurium* and 99% ΔTTSS-1, 10% wild type *S. typhimurium* and 90% ΔTTSS-1, 50% wild type *S. typhimurium* and 50% ΔTTSS-1, or 100% wild type *S. typhimurium*, as indicated. An additional control infection was performed with 5 * $10^5$ bacteria (100% wild type *S. typhimurium*; 5 mice; marked as *). The wild type *S. typhimurium* strain (M939) was marked with a kanamycin resistance cassette integrated downstream of the *sopE* gene. This allowed quantifying wild type *S. typhimurium* (kan$^{resistant}$) and ΔTTSS-1 (kan$^{sensitive}$) in the inoculum (data not shown) and in the gut lumen (see, below).

The mice were sacrificed at day 1 post infection and we analyzed the following parameters: (a; suppl. Fig. 1a) Total colonization levels by wild type *S. typhimurium* (M939; kan$^{resistant}$; white boxes) and ΔTTSS-1 (SB161; kan$^{sensitive}$; grey boxes) in the gut lumen. The densities (cfu/gram) were determined by plating appropriate dilutions of the cecal contents on McConkey agar plates harboring kanamycin (50μg/ml) or not. These data verified that the mixed inoculum approach was successful in adjusting the absolute density of wild type *S. typhimurium* in the gut lumen of the infected mice. (b; suppl. Fig. 1b). The gut inflammation was analyzed using hematoxilin and eosin stained cecum tissue sections and a scoring scheme as described previously [37]. These data verified that the intensity of gut inflammation increased with an increasing fraction of wild type *S. typhimurium* present in the gut lumen.

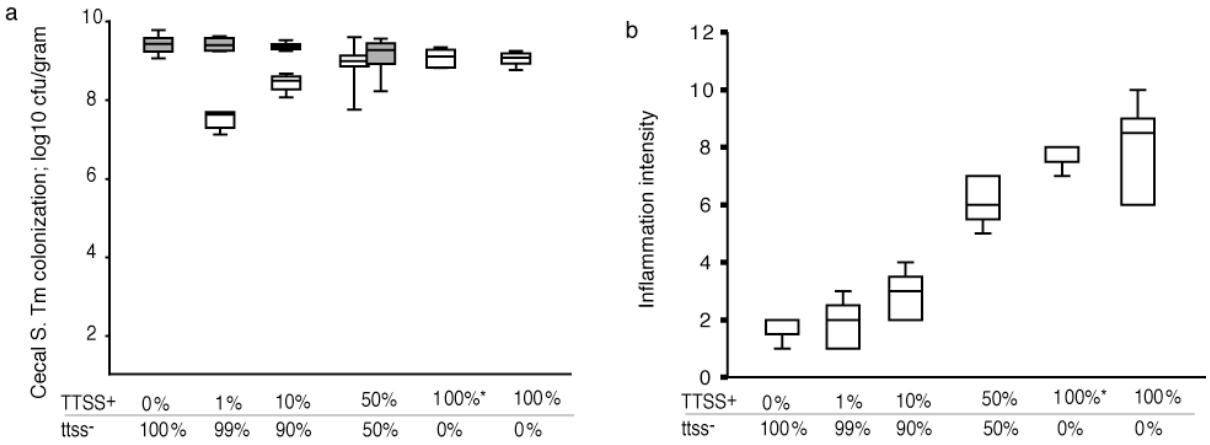


**Supplementary Figure 1**

**a**, Infections with mixtures of wild type *S. typhimurium* and increasing fractions of ΔTTSS-1 result in a proportional decrease in the total number of bacteria expressing the TTSS-1$^{+}$ phenotype in the gut lumen. Total colonization levels by wild type *S. typhimurium* (M939; kan$^{resistant}$; white boxes) and ΔTTSS-1 (SB161; kan$^{sensitive}$; grey boxes) in the gut lumen are indicated. Gut inflammation levels decrease with decreasing proportions of wildtype *S. typhimurium* that are capable of expressing the TTSS-1$^{+}$ phenotype. The data are the same as depicted in Figure 2d, but includes the additional control group infected with 5 * $10^{5}$ wild type *S. typhimurium* (marked as *). This control demonstrates that, in the absence of any ΔTTSS-1 bacteria, wild type *S. typhimurium* always grows up to densities of approx. $10^{9}$ cfu/g cecum content, irrespective of the absolute size of the original inoculum.

## Experiment 3. Killing of *S. typhimurium* in gut tissues by key innate immune defenses in a mouse infection experiment (Figure 2f of the paper and suppl Fig. S2).

Bacteria that have invaded into intestinal tissues are killed by innate immune mechanisms which generate antibacterial nitrogen- and oxygen radicals (iNOS and NADPH-oxidase; gp91-phox protein of the phagocytic **NADPH** oxidase). It has been shown previously that mice lacking these key anti-bacterial defense systems cannot restrict pathogen growth in various infection models[39]. Thus, comparing *S. typhimurium* tissue loads in wild type and *Cybb/NOS2* knockout mice allows estimating the extent of bacterial killing in infected gut tissues.

Streptomycin treated wild type mice (n = 5 C57BL/6 mice per group) or *Cybb/NOS2* knockout mice (n = 5 mice per group, C57BL/6 genetic background; bred in the same colony

as the wild type control mice) were infected with wild type *S. typhimurium* ($5 * 10^7$ bacteria, intragastrically). *Cybb/NOS2* double knockout mice were generated by crossing B6.129S6-*Cybb*$^{tm1Din}$/J[40] and B6;129P2-*Nos2*$^{tm1Lau}$/J[41] (both from Jackson Laboratory). The bacteria harbored a GFP reporter plasmid (pM973;[38]) allowing the quantification of *S. typhimurium* loads in the infected gut tissue. The mice were sacrificed at day 2 post infection and we analyzed the following parameters: (a; suppl. Fig. 2a) Total colonization levels by wild type *S. typhimurium* in the cecum lumen[34]. The densities (cfu/gram) were determined by plating appropriate dilutions of the cecal contents on McConkey agar plates. Colonization densities in the gut lumen did not differ significantly between both groups of mice (p=0.730; Mann Whitney U-test) (b; suppl. Fig. 2b) The gut inflammation was analyzed using hematoxilin and eosin stained cecum tissue sections and a scoring scheme as described previously[37]. Inflammation was pronounced and did not differ significantly between both groups of mice (p=0.484; Mann Whitney U-test).

Significant differences were detected in the numbers of *S. typhimurium* bacteria present in the cecum tissues of both groups of mice. These data are depicted in Fig. 2f and were generated in the following way: The cecal tissue was fixed and cryo-embedded as described[38] and 20µm thick cryo-sections were stained with phalloidin-TRITC (stains actin; red fluorescence) and DAPI (stains DNA, blue fluorescence). All bacteria (expressing GFP-reporter of pM973) present in the gut tissue on one tissue section were enumerated. At least 3 tissue sections were analyzed per mouse.

These data indicate that the innate immune system effectively kills approximately 90% of all bacteria entering the gut tissue. This suggests that host tissue invasion by *S. typhimurium* can be considered as a self-destructive act.

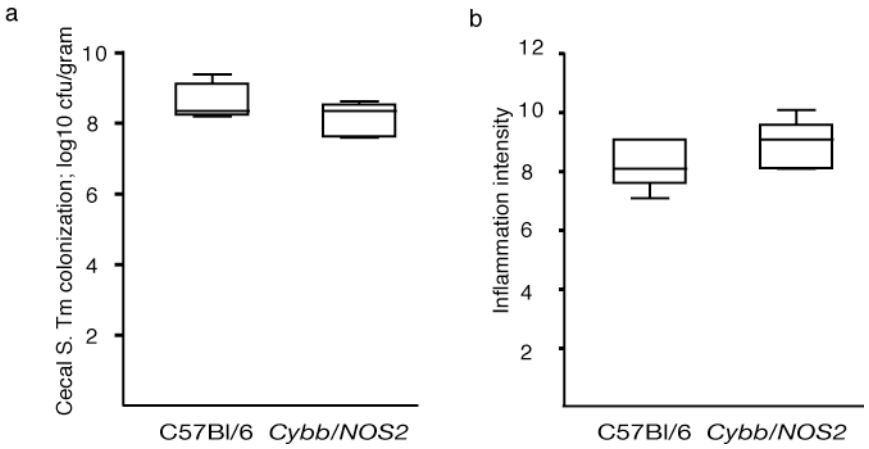


**Supplementary Figure 2**

**a,** Density of *S. typhimurium* in the gut lumen, and **b**, inflammation intensity were very similar between wild type mice (C57BI/6) and *Cybb/NOS2* knock-out mice.

## References

30. Hofbauer, J. & Sigmund, K. Evolutionary Games and Population Dynamics, (Cambridge University Press, 1998).

31. Hauert, C., Michor, F., Nowak, M.A. & Doebeli, M. Synergy and discounting of cooperation in social dilemmas. Journal of Theoretical Biology 239, 195-202 (2006).

32. Schlumberger, M.C. et al. Real-time imaging of type III secretion: Salmonella SipA injection into host cells. *Proceedings of the National Academy of Sciences of the United States of America* **102**, 12548-12553 (2005).

33. Hautefort, I., Proenca, M.J. & Hinton, J.C.D. Single-copy green fluorescent protein gene fusions allow accurate measurement of Salmonella gene expression in vitro and during infection of mammalian cells. *Applied and Environmental Microbiology* **69**, 7480-7491 (2003).

34. Barthel, M. et al. Pretreatment of Mice with Streptomycin Provides a Salmonella enterica Serovar Typhimurium Colitis Model That Allows Analysis of Both Pathogen and Host. *Infection and Immunity* **71**, 2839 (2003).

35. Hapfelmeier, S. & Hardt, W.D. A mouse model for S. typhimurium-induced enterocolitis. *Trends in Microbiology* **13**, 497-503 (2005).

36. Hapfelmeier, S. et al. Microbe sampling by mucosal dendritic cells is a discrete, MyD88-independent step in {Delta} invG S. Typhimurium colitis. *Journal of Experimental Medicine* **205**, 437 (2008).

37. Stecher, B. et al. Salmonella enterica Serovar Typhimurium Exploits Inflammation to Compete with the Intestinal Microbiota. *PLoS Biology* **5**, e244 (2007).

38. Hapfelmeier, S. et al. The Salmonella Pathogenicity Island (SPI)-2 and SPI-1 Type III Secretion Systems Allow Salmonella Serovar typhimurium to Trigger Colitis via MyD88-Dependent and MyD88-Independent Mechanisms 1. *The Journal of Immunology* **174**, 1675-1685 (2005).

39. Vazquez-Torres, A. & Fang, F.C. Oxygen-dependent anti-Salmonella activity of macrophages. *Trends in Microbiology* **9**, 29-33 (2001).

40. Pollock, J.D. et al. Mouse model of X–linked chronic granulomatous disease, an inherited defect in phagocyte superoxide production. *Nature Genetics* **9**, 202-209 (1995).

41. Laubach, V.E., Shesely, E.G., Smithies, O. & Sherman, P.A. Mice Lacking Inducible Nitric Oxide Synthase are Not Resistant to Lipopolysaccharide-Induced Death. *Proceedings of the National Academy of Sciences of the United States of America* **92**, 10688-10692 (1995).